NONLOCAL TRANSPORT OF PASSIVE SCALAR IN TURBULENT CHANNEL FLOW

Fujihiro Hamba
Institute of Industrial Science,
University of Tokyo
Komaba, Meguro-ku, Tokyo 153-8505, Japan
hamba@iis.u-tokyo.ac.jp

ABSTRACT

A nonlocal expression for the scalar flux was derived using the Green's function for the scalar. The nonlocal diffusivity in the expression represents a contribution to the scalar flux from the mean scalar gradient at remote points in space and time. Direct numerical simulation (DNS) of channel flow was carried out to validate the nonlocal expression. The velocity and scalar fields as well as the Green's function were calculated in the cases of the one- and two-dimensional mean scalar. It was shown that the nonlocal expression exactly holds in both cases. The local expression for the scalar flux was also examined to show that the local approximation is not accurate enough and that nonlocal effects are important. The nonlocal expression evaluated in DNS is expected to gain insight into modeling the scalar transport.

INTRODUCTION

Modeling the turbulent transport of scalars such as mass, heat, and concentration is an important problem in many fields including engineering and geophysics. The scalar flux needs to be evaluated to solve the equation for the mean scalar. In the eddy diffusivity model the scalar flux is assumed to be proportional to the scalar gradient and to be directed down the gradient. Although this model is widely used, the limitation of this approximation was also pointed out; a gradient transport model requires the characteristic scale of the transport mechanism must be small compared with the distance over which the mean gradient of the transported property changes appreciably (Corrsin, 1974). In turbulent flows the length scale of turbulence is often as large as that of the mean field variation. One of typical examples is the scalar transport in the atmospheric boundary layer; convective eddies driven by buoyancy are as large as the boundary layer height and the eddy diffusivity model has some defects.

Since the nonlocal effect is important in the atmospheric boundary layer several attempts have been done to develop nonlocal models. Stull (1984) proposed the transilient turbulence theory that describes nonlocal transport using a matrix of mixing coefficients. Berkowicz and Prahm (1980) proposed a generalization of the eddy diffusivity; that is, the scalar flux is expressed by a spatial integral of the scalar gradient. The nonlocal diffusivity involved in the model represents a contribution to the scalar flux from the scalar gradient at remote points. Nakayama et al. (1988) applied this model to the calculation of the scalar field in the turbulent boundary layer for engineering problems. Using the Green's function Hamba (1995) obtained a exact nonlocal expression for the scalar flux and evaluated one-dimensional profiles of the nonlocal diffusivity from the LES of the atmospheric boundary layer.

In the atmospheric boundary layer turbulent motion is driven by buoyancy. Since in many other flows turbulence is produced by mean shear, it is interesting to examine nonlocal effects in shear turbulence. In this work we examine a channel flow as a basic example of shear turbulence. Using the Green's function we derive an exact nonlocal expression for the scalar flux. We carry out a DNS to evaluate one- and two-dimensional profiles of the nonlocal diffusivity. We examine the limitation of the local approximation and the importance of nonlocal effects.

FORMULATION

In order to solve the transport equation for the mean scalar it is necessary to model the scalar flux. In the eddy diffusivity model widely used, the scalar flux is approximated by

$$\langle u_i'\theta' \rangle = -\kappa_T \frac{\partial \Theta}{\partial x_i} \qquad (1)$$

Here, $\langle\ \rangle$ denotes the ensemble average, Θ is the mean scalar, u'_i and θ' are the velocity and scalar fluctuations, respectively, and κ_T is the eddy diffusivity. This model is local in space in the sense that the scalar flux at a point is expressed in terms of physical quantities at the same point. Berkowicz and Prahm (1980) proposed a

generalization of the eddy diffusivity model; the scalar flux is given by

$$\langle v'\theta'\rangle(y) = -\int dy' \kappa_{NL}(y;y') \frac{\partial \Theta(y')}{\partial y'} \qquad (2)$$

where κ_{NL} is a coefficient representing a nonlocal contribution; hereafter we refer to it as the nonlocal eddy diffusivity.

Hamba (1995) introduced the Green's function to obtain an explicit exact expression for the scalar flux. The equation for the Green's function for θ' is given by

$$\frac{\partial g_i'}{\partial t} + u_j \frac{\partial g_i'}{\partial x_j} - \frac{\partial}{\partial x_j}\langle u_j' g_i'\rangle - \kappa \frac{\partial^2 g_i'}{\partial x_j \partial x_j} = u_i' \delta(\mathbf{x}-\mathbf{x}')\delta(t-t') \qquad (3)$$

where κ is the molecular diffusivity. Using g'_i the formal solution for the scalar fluctuation can be written as

$$\theta'(\mathbf{x},t) = -\int d\mathbf{x}' \int_0^t dt' g_i'(\mathbf{x},t;\mathbf{x}',t') \frac{\partial}{\partial x_i'} \Theta(\mathbf{x}',t') \qquad (4)$$

This solution leads to the scalar flux expression with the nonlocal eddy diffusivity as follows

$$\langle u_i'\theta'\rangle(\mathbf{x},t) = -\int d\mathbf{x}' \int_0^t dt' \kappa_{NLij}(\mathbf{x},t;\mathbf{x}',t') \frac{\partial}{\partial x_j'} \Theta(\mathbf{x}',t') \quad \left(\equiv \langle u_i'\theta'\rangle_{NL}\right) \qquad (5)$$

where

$$\kappa_{NLij}(\mathbf{x},t;\mathbf{x}',t') = \langle u_i'(\mathbf{x},t) g_j'(\mathbf{x},t;\mathbf{x}',t')\rangle \qquad (6)$$

Let us mention the relation of the nonlocal expression (5) to the local approximation. If the scalar gradient $\partial\Theta/\partial x'_i$ is nearly constant in the region where $\kappa_{NLij} \neq 0$, the scalar flux can be approximated by

$$\langle u_i'\theta'\rangle \cong -\kappa_{Lij} \frac{\partial \Theta}{\partial x_j} \left(\equiv \langle u_i'\theta'\rangle_L\right) \qquad (7)$$

where κ_{Lij} is the local eddy diffusivity defined as

$$\kappa_{Lij}(\mathbf{x},t) = \int d\mathbf{x}' \int_0^t dt' \kappa_{NLij}(\mathbf{x},t;\mathbf{x}',t') \qquad (8)$$

Therefore, whether the local approximation is good or not depends on the relation in the length and time scales between κ_{NL} and $\partial\Theta/\partial x'_i$.

RESULTS AND DISCUSSION

In this section we show results from the DNS of channel flow. Using DNS data we examine the following two points: whether the nonlocal expression (5) is exact or not and how good is the local approximation given by (7). In the DNS we numerically solve the equations for the velocity and the scalar given by

Table 1: Parameters for three runs.

Case	θ_b	f_θ	Average
1	0	2	x, z, t
2	0	$\exp(-y^2/0.09)$	x, z, t
3	$\sin(4\pi x/L_x)$	0	z, t

$$\frac{\partial u_i}{\partial t} = -u_j \frac{\partial u_i}{\partial x_j} - \frac{\partial p}{\partial x_i} + \nu \frac{\partial^2 u_i}{\partial x_j \partial x_j} + f_u \delta_{i1} \qquad (9)$$

$$\frac{\partial u_i}{\partial x_i} = 0 \qquad (10)$$

$$\frac{\partial \theta}{\partial t} = -u_i \frac{\partial \theta}{\partial x_i} + \kappa \frac{\partial^2 \theta}{\partial x_i \partial x_i} + f_\theta \qquad (11)$$

respectively, where p is the pressure, ν is the molecular viscosity, f_u is an external force, and f_θ is an external source. The equation for the Green's function g'_i given by (3) is also solved. The variables $x_1(=x)$, $x_2(=y)$, and $x_3(=z)$ denote the streamwise, wall-normal, and spanwise directions, respectively; corresponding velocity components are given by $u_1(=u)$, $u_2(=v)$, and $u_3(=w)$. Hereafter, all variables except for θ are nondimensionalized by the wall-friction velocity u_τ and the channel half width $L_y/2$. Since θ is linear in the equations, it can be normalized arbitrarily.

The Reynolds number based on u_τ and $L_y/2$ is set to $Re_\tau=180$ and the Prandtl number is $Pr=0.7$. The size of the computational domain is $L_x \times L_y \times L_z = 9.6 \times 2 \times 4.8$. A staggered grid is adopted; it is uniform in the x and z directions and is stretched in the y direction using a hypertangent function. The number of the grid points is $N_x \times N_y \times N_z = 256 \times 128 \times 256$. The periodic boundary conditions for u_i, θ, and g'_i are used in the x and z directions. The no-slip condition $u_i=0$ is imposed at the wall (y=-1,y=1). The upper-wall boundary condition for the scalar is $\theta=0$ whereas the lower-wall condition is $\theta=\theta_b(x,t)$; the function will be described later. The wall boundary condition for the Green's function is $g'_i=0$ because the boundary condition for the scalar is of the Dirichlet type. We use the second-order finite-difference scheme in space and the Adams-Bashforth method for time marching. The computational time step is $\Delta t = 1.5\times10^{-4}$. The computation was run for a sufficiently long time to be statistically independent of the initial condition; then statistics such as the scalar flux were accumulated over a time period of 18 unless otherwise mentioned.

We calculated three cases as shown in Table 1. In all cases the same velocity field is used; it is a typical channel flow statistically steady in time and homogeneous in the x and z directions. In Cases 1 and 2 the scalar at the lower wall is set to $\theta_b=0$. Instead, the source term is nonzero; it is set to $f_\theta=2$ in the whole region in Case 1 whereas it is concentrated near the center line at y=0 in Case 2. In Case 3 the source term is set to zero and the dependence of θ_b on space is introduced. θ_b is periodic in x with the period of $L_x/2$; two cycles are included in the computational domain at $0<x<L_x$.

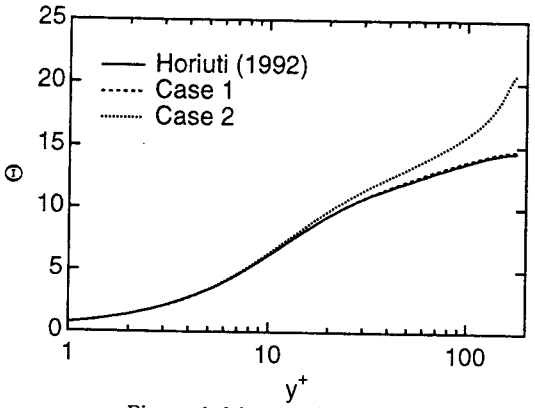

Figure 1. Mean scalar profiles.

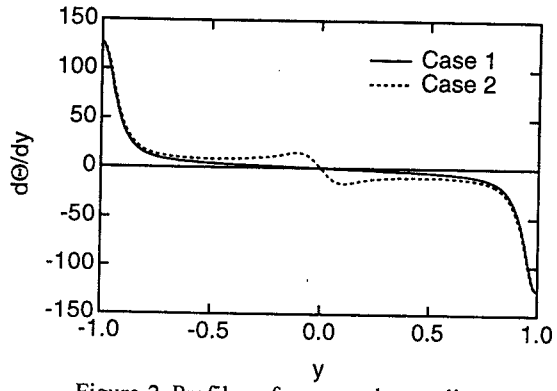

Figure 2. Profiles of mean scalar gradient.

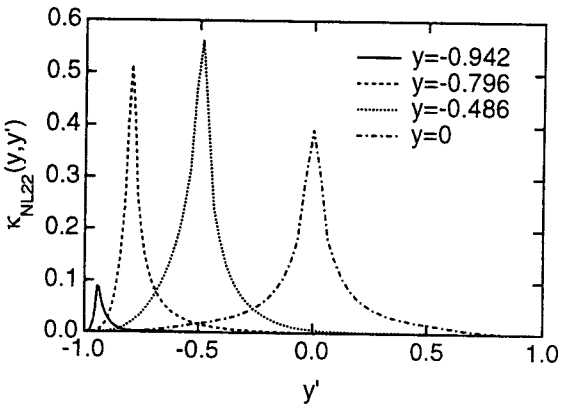

Figure 3. Profiles of nonlocal diffusivity κ_{NL22}.

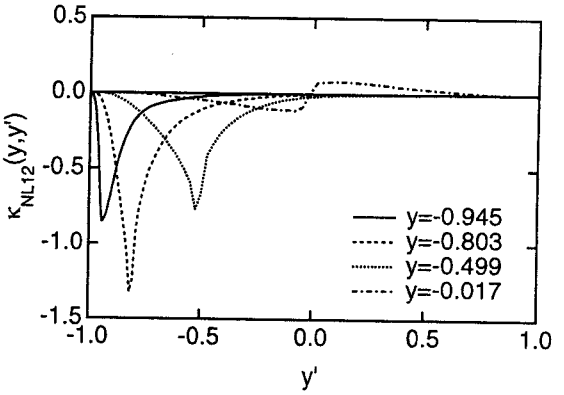

Figure 4. Profiles of nonlocal diffusivity κ_{NL12}.

Since the source term f_θ in Cases 1 and 2 is a function of y only, the scalar field is statistically homogeneous in the x and z directions like the velocity field. We take an average over the x-z plane and in time; statistics depend only on y. In this case the scalar flux given by (5) can be expressed as

$$\langle u_i'\theta'\rangle_{NL}(y) = -\int dy' \kappa_{NLi2}(y;y') \frac{\partial \Theta(y')}{\partial y'} \qquad (12)$$

$$\kappa_{NLi2}(y;y') = \int dx' \int dz' \int_0^t dt' \langle u_i'(\mathbf{x},t) g_2'(\mathbf{x},t;\mathbf{x}',t') \rangle \qquad (13)$$

because the scalar gradient $\partial\Theta/\partial y'$ does not depend on x', z', or t'. The scalar flux given by (7) is also expressed as

$$\langle u_i'\theta'\rangle_L(y) = -\kappa_{Li2}(y) \frac{\partial \Theta}{\partial y} \qquad (14)$$

$$\kappa_{Li2}(y) = \int dy' \kappa_{NLi2}(y;y') \qquad (15)$$

Figure 1 shows the mean scalar profiles for Cases 1 and 2. The DNS result by Horiuti (1992) is also shown; he carried out the DNS of scalar in channel flow with the same parameters as Case 1. The agreement between Case 1 and the DNS by Horiuti (1992) is good. The mean scalar in Case 1 shows a logarithmic profile like the mean velocity because both fields have a force or source term constant in space. On the other hand, in Case 2 the source term is concentrated near the center line; the scalar shows a steep gradient near $y^+=180$ where y^+ is the wall-unit coordinate. As previously mentioned, to examine the nonlocal effect we need to compare the length scale of κ_{NLi2} and that of the scalar gradient. Figure 2 shows the profiles of the scalar gradient in linear scale for Cases 1 and 2. The scalar gradient rapidly decreases near the wall in both cases. It gradually changes at $-0.8<y<0.8$ in Case 1 whereas it rapidly decreases near y=0 in Case 2. The length scale of the scalar gradient variation near y=0 in Case 2 is much shorter than that in Case 1.

Figures 3 and 4 show the profiles of the nonlocal diffusivity κ_{NL22} and κ_{NL12}, respectively, as functions of y' for four locations of y. The components κ_{NL22} and κ_{NL12} are involved in $\langle v'\theta'\rangle$ and $\langle u'\theta'\rangle$, respectively. The profiles represent the contribution of the scalar gradient at y' to the scalar flux at a given point of y. In Fig. 3 the profile of κ_{NL22} becomes wider as y increases. Here, let us evaluate the width of the profile as the distance between the two points whose value is e^{-1} times the peak value; the width is 0.05 for y=-0.942 and 0.12 for y=0. The profile of κ_{NL22} for the atmospheric boundary layer was obtained by Hamba (1995); the width is $0.49y_b$ for $y=0.6y_b$ where y_b is the boundary layer height. The profiles of κ_{NL22} for the channel flow are not as wide as those for the atmospheric boundary layer. This is due to the difference in the mechanism of turbulence production. In the atmospheric boundary layer plumes produced near the bottom surface rise to the upper boundary; the turbulent field can be nonlocal in the vertical direction.

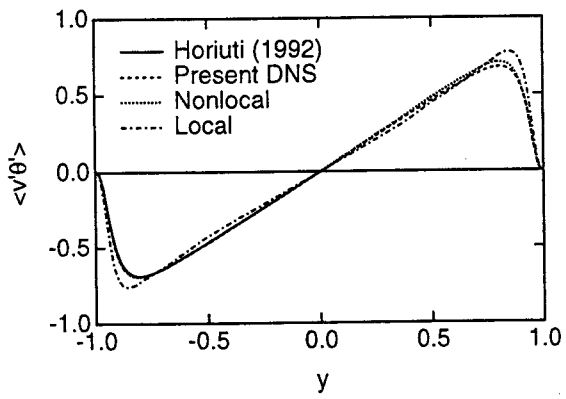

Figure 5. Profiles of scalar flux $\langle v'\theta' \rangle$ for Case 1.

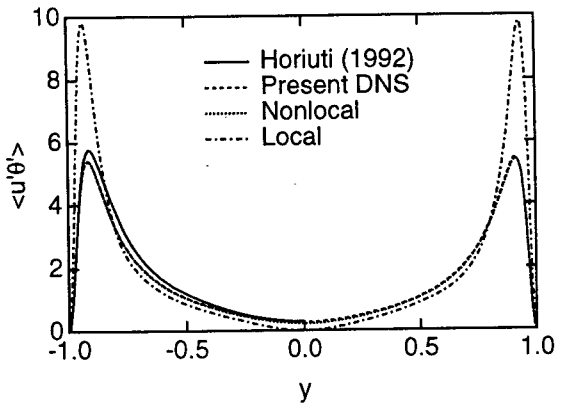

Figure 6. Profiles of scalar flux $\langle u'\theta' \rangle$ for Case 1.

On the other hand, in the channel flow vortices produced by mean shear are stretched in the streamwise direction; the nonlocal effect in the wall-normal direction is not very strong. Nevertheless, the profiles in the channel flow cannot be approximated by $\delta(y'-y)$; some nonlocal effect may remain and its strength is determined by the relation between the width of the nonlocal diffusivity and the length scale of the mean field variation. In Fig. 3 the location of the peak corresponds to $y'=y$. This means that the contribution of the scalar gradient at the same point is the largest. The peak value may be proportional to $\langle v'^2 \rangle$.

In Fig. 4 the value of κ_{NL12} is negative except for the case of $y=-0.017$ since the $\langle u'\theta' \rangle$ is negative at $-1<y<0$. The profile of κ_{NL12} is somewhat wider than that of κ_{NL22} at the corresponding location of y. For example, the width of κ_{NL12} is 0.12 for $y=-0.945$. The profile of κ_{NL12} for $y=-0.017$ is different from the other three profiles; it is negative at the lower half ($-1<y'<0$) and positive at the upper half ($0<y'<1$). Although the absolute value is small the profile shows fairly nonlocal contribution. Here, we should note that the value of κ_{NLi2} is common for Cases 1 and 2 because it is determined solely by the velocity field and it does not depend on the specific mean scalar field.

Then, we examine the profiles of the scalar flux for Case 1. Figure 5 shows the profiles of $\langle v'\theta' \rangle$. At the lower half in Fig. 5 the DNS by Horiuti, the present DNS, and the nonlocal expression $\langle v'\theta' \rangle_{NL}$ agree well with each other.

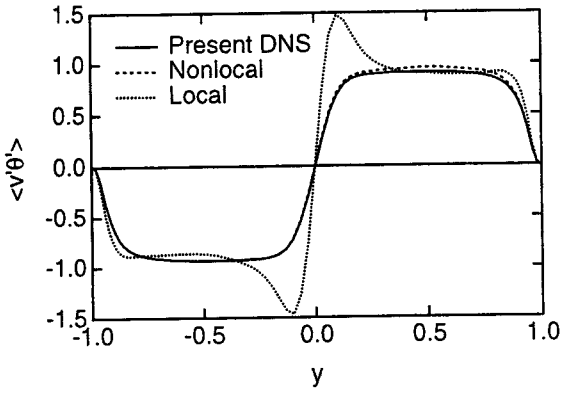

Figure 7. Profiles of scalar flux $\langle v'\theta' \rangle$ for Case 2.

The absolute value of $\langle v'\theta' \rangle_L$ is somewhat greater than the DNS result at $y=-0.9$; it is slightly smaller than the DNS away from the wall. Figure 6 shows the profiles of $\langle u'\theta' \rangle$ for Case 1. The value of $\langle u'\theta' \rangle$ by the present DNS is slightly less than that of the DNS by Horiuti (1992). Here, we consider the present DNS is correct when comparing it with the eddy diffusivity expressions because their coefficients are evaluated using the present DNS data. The nonlocal expression $\langle u'\theta' \rangle_{NL}$ agrees well with the DNS result. On the other hand, $\langle u'\theta' \rangle_L$ is much greater than the DNS result near the wall. The overestimate of $\langle u'\theta' \rangle_L$ is larger than that of $\langle v'\theta' \rangle_L$. This is because the profile of κ_{NL12} near the wall in Fig. 4 is wider than that of κ_{NL22} in Fig. 3 and the nonlocal effect is more important. Near the center line at $y=0$, $\langle u'\theta' \rangle_L$ vanishes although the DNS result remains to be a small positive value. This zero value of $\langle u'\theta' \rangle_L$ is because $\partial\Theta/\partial y=0$. As shown in Fig. 4 the nonlocal diffusivity has a broad profile for $y=0$. Since the scalar gradient changes its sign at $y=0$ the contributions of the upper and lower halves in (12) are both positive; they induce a positive scalar flux at $y=0$.

To demonstrate that the nonlocal diffusivity is independent of the mean scalar field, we adopt another type of f_0 concentrated near $y=0$ in Case 2. In Fig. 7 $\langle v'\theta' \rangle_{NL}$ agrees well with the DNS result. On the other hand, the absolute value of $\langle v'\theta' \rangle_L$ is much greater than the DNS result near the center line. This overestimate is due to the short length scale of the mean field variation in Case 2 as shown in Fig. 2. The agreement between $\langle u'_i\theta' \rangle_{NL}$ and the DNS result in both Cases 1 and 2 demonstrates that the nonlocal expression (12) is exact in the case of the one-dimensional mean scalar.

Next, we investigate the nonlocal contribution not only in the wall-normal direction but also in the streamwise direction. In Case 3 the value of the scalar at the lower wall, θ_b, is set to be periodic in x; the resulting scalar field is statistically homogeneous only in the z direction. We take an average in the z direction and in time; statistics depend on x and y. In this case the scalar flux given by (5) can be expressed as

$$\langle u'_i\theta' \rangle_{NL}(x,y) = -\int dx' \int dy' [\kappa_{NLi1}(x,y;x',y') \frac{\partial}{\partial x'} \Theta(x',y')$$

$$+\kappa_{NLi2}(x,y;x',y') \frac{\partial}{\partial y'} \Theta(x',y')] \qquad (16)$$

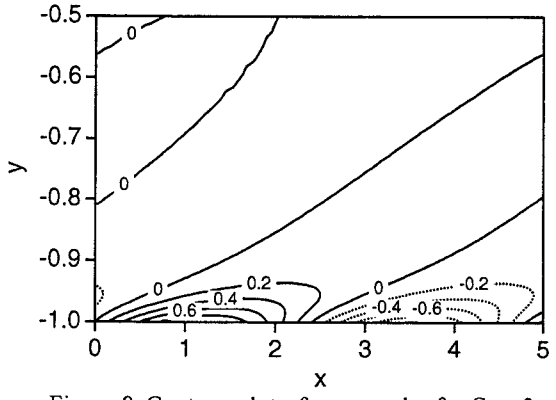

Figure 8. Contour plot of mean scalar for Case 3.

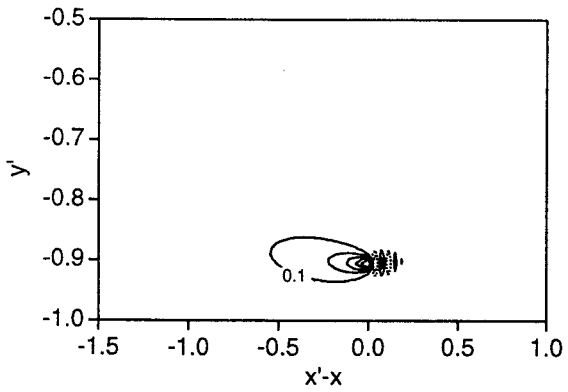

Figure 9. Contour plot of nonlocal diffusivity κ_{NL22} for y=-0.901 for Case 3.

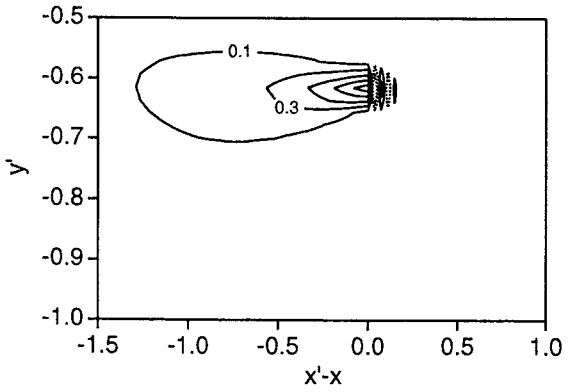

Figure 10. Contour plot of nonlocal diffusivity κ_{NL22} for y=-0.605 for Case 3.

$$\kappa_{NLij}(x,y;x',y') = \int dz' \int_0^t dt' \langle u_i'(\mathbf{x},t) g_j'(\mathbf{x},t;\mathbf{x}',t') \rangle \quad (17)$$

Since the velocity field is homogeneous in the x direction and inhomogeneous in the y direction, the diffusivity $\kappa_{NLij}(x,y;x',y')$ is a function of x'-x, y, and y'. The scalar flux given by (7) is also expressed as

$$\langle u_i'\theta' \rangle_L(x,y) = -\kappa_{Li1}(x,y)\frac{\partial \Theta}{\partial x} - \kappa_{Li2}(x,y)\frac{\partial \Theta}{\partial y} \quad (18)$$

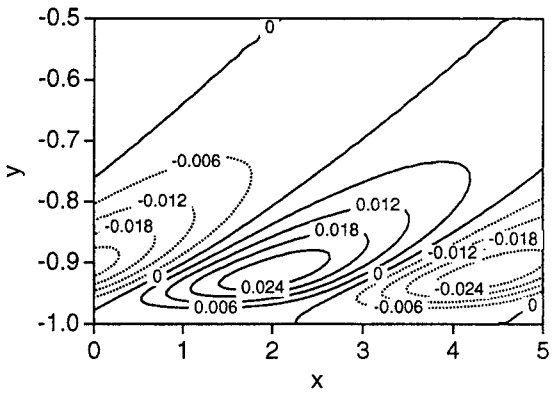

Figure 11. Contour plot of scalar flux $\langle v'\theta' \rangle$ for Case 3.

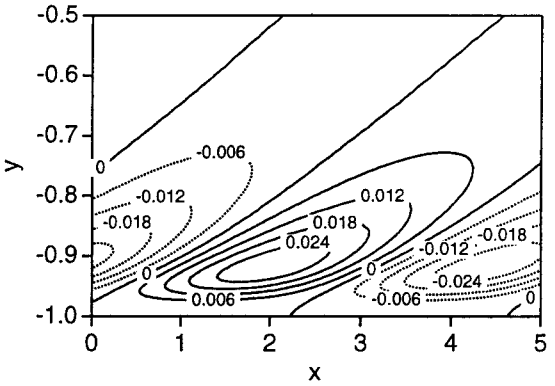

Figure 12. Contour plot of scalar flux $\langle v'\theta' \rangle_{NL}$ for Case 3.

$$\kappa_{Lij}(x,y) = \int dx' \int dy' \kappa_{NLij}(x,y;x',y') \quad (19)$$

Figure 8 shows the two-dimensional contour plot of the mean scalar for Case 3. About the half region in the x direction is shown. At the lower wall Θ is positive at $0<x<2.4$ and negative at $2.4<x<4.8$. The absolute value of the mean scalar near the wall decreases rapidly as y increases because the source term f_θ is zero in this case. The scalar gradient in the y direction is greater than that in the x direction. Away from the wall the phase of the variation in the x direction is shifted downstream due to the effect of convection by the mean flow.

Figures 9 and 10 show the contour plots of κ_{NL22} as functions of x'-x and y' for y=-0.901 and y=-0.605, respectively. The diffusivity κ_{NL22} represents the contribution of the scalar gradient $\partial\Theta/\partial y$ at (x'-x,y') to the scalar flux $\langle v'\theta' \rangle$ at (0,y). The profiles are elongated in the upstream direction due mainly to the mean flow convection. The elongated profiles imply that the scalar gradient at points apart in the upstream direction affect the scalar gradient at (0,y). The size in this direction is longer for y=-0.605 than for y=-0.901. This difference is because the mean flow is faster and the time scale k/ε is greater for y=-0.605. The width in the y direction reflects the turbulent diffusion as examined before. Some wiggle is seen just downstream the point at (0,y). Although some nonlocal contribution due to the diffusion may exist even from downstream, the reason for the wiggle is not

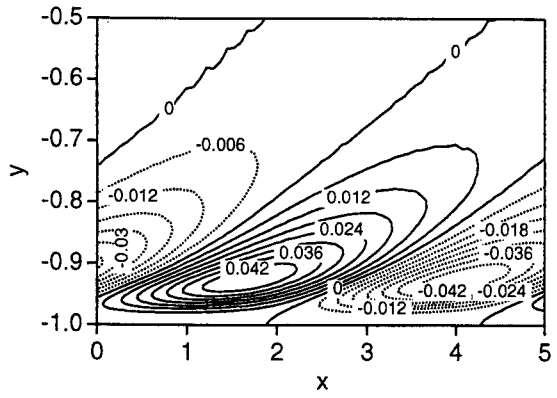

Figure 13. Contour plot of scalar flux $\langle v'\theta' \rangle_L$ for Case 3.

clear; it may be due to the error of the finite different scheme.

Figures 11, 12, and 13 show the contour plots of $\langle v'\theta' \rangle$ by the DNS, $\langle v'\theta' \rangle_{NL}$, and $\langle v'\theta' \rangle_L$, respectively. The value of $\langle v'\theta' \rangle_{NL}$ agrees well with the DNS result whereas the absolute value of $\langle v'\theta' \rangle_L$ is fairly greater than the DNS near the wall. Moreover, the location of the peak of $\langle v'\theta' \rangle_L$ in Fig. 13 is shifted upstream compared to the DNS result; the positive peak of $\langle v'\theta' \rangle_L$ is located at (1.7,-0.93) whereas that of the DNS result is at (2.0,-0.92). In the local expression the scalar flux takes its maximum value at the point where the scalar gradient is the largest when the local diffusivity is constant. This result indicates that in the DNS the peak location of the scalar flux is shifted downstream compared to that of the scalar gradient. This phenomena cannot be described by the local expression; the nonlocal expression is required to predict the peak location accurately.

CONCLUSIONS

A nonlocal expression for the scalar flux is derived using the Green's function for the scalar. The nonlocal diffusivity represents the contribution to the scalar flux from the scalar gradient at remote points in space and time. To validate the nonlocal expression DNS of channel flow is carried out; the velocity and scalar fields and the Green's function are calculated in the cases of the one- and two-dimensional mean scalar. It was shown that the nonlocal expression is exact in all cases. At the same time the local expression for the scalar flux is compared; the scalar flux near the wall is overestimated and the peak location is shifted in the streamwise direction compared to the DNS results. This shows that the local approximation is not accurate enough and nonlocal effects are important. The nonlocal expression evaluated in the DNS is expected to gain insight into modeling the scalar flux.

As future work, this approach should be applied to more complex flows than channel flow; it is interesting to examine two-dimensional or temporally changing mean velocity field and its effect on the scalar flux. We expect that this approach can also be applied to the Reynolds stress; the nonlocal viscosity represents the nonlocal contribution of the velocity gradient to the Reynolds stress.

REFERENCES

Berkowicz, R., and Prahm, L. P., 1980, "On the spectral turbulent diffusivity theory for homogeneous turbulence," *J. Fluid Mech.*, Vol. 100, pp. 433-448.

Corrsin, S., 1974, "Limitations of gradient transport models in random walks and in turbulence," *Advances in Geophysics*, Vol. 18A, pp. 25-60.

Hamba, F., 1995, "An analysis of nonlocal scalar transport in the convective boundary layer using the Green's function," *J. Atmos. Sci.*, Vol. 52, pp. 1084-1095.

Horiuti, K., 1992, "Assessment of two-equation models of turbulent passive-scalar diffusion in channel flow," *J. Fluid Mech.*, Vol. 238, pp. 405-433.

Nakayama, A., Nguyen, H. D., and Daif, M. B., 1988, "Nonlocal diffusion model in turbulent boundary layer," *Proc. Third Int. Symp. on Refined Flow Modeling and Turbulence Measurements*, Int. Assoc. Hydraulic Res., Tokyo, pp. 305-312.

Stull, R. B., 1984, "Transilient turbulence theory. Part I: The concept of eddy mixing across finite distances," *J. Atmos. Sci.*, Vol. 41, pp. 3351-3367.